PGC1α expression is controlled in skeletal muscles by PPARβ, whose ablation results in fiber-type switching, obesity, and type 2 diabetes

Michael Schuler,[1,2,3,4,5,6] Faisal Ali,[1,2,3,4,5] Céline Chambon,[1,2,3,4,5] Delphine Duteil,[1,2,3,4,5] Jean-Marc Bornert,[1,2,3,4,5] Aubry Tardivel,[7] Béatrice Desvergne,[7] Walter Wahli,[7] Pierre Chambon,[1,2,3,4,5,6,*] and Daniel Metzger[1,2,3,4,5,6,*]

[1] IGBMC (Institut de Génétique et de Biologie Moléculaire et Cellulaire), Department of Physiological Genetics
[2] Inserm, U596
[3] CNRS, UMR7104
[4] Collège de France
Illkirch, F-67400 France
[5] Université Louis Pasteur, Strasbourg, F-67000 France
[6] Institut Clinique de la Souris, 67404, Illkirch, Strasbourg, France
[7] Center for Integrative Genomics, National Center of Competence in Research "Frontiers in Genetics," University of Lausanne, CH-1015 Lausanne, Switzerland
*Correspondence: metzger@igbmc.u-strasbg.fr (D.M.), chambon@igbmc.u-strasbg.fr (P.C.)

Summary

Mice in which peroxisome proliferator-activated receptor β (PPARβ) is selectively ablated in skeletal muscle myocytes were generated to elucidate the role played by PPARβ signaling in these myocytes. These somatic mutant mice exhibited a muscle fiber-type switching toward lower oxidative capacity that preceded the development of obesity and diabetes, thus demonstrating that PPARβ is instrumental in myocytes to the maintenance of oxidative fibers and that fiber-type switching is likely to be the cause and not the consequence of these metabolic disorders. We also show that PPARβ stimulates in myocytes the expression of PGC1α, a coactivator of various transcription factors, known to play an important role in slow muscle fiber formation. Moreover, as the PGC1α promoter contains a PPAR response element, the effect of PPARβ on the formation and/or maintenance of slow muscle fibers can be ascribed, at least in part, to a stimulation of PGC1α expression at the transcriptional level.

Introduction

Skeletal muscles account for up to 55% of total body mass in nonobese mammals and generate motile forces and heat. They are a major site for carbohydrate and fatty acid metabolism and are composed of three myofiber types exhibiting distinct contractile and metabolic properties: (1) slow-twitch, oxidative, fatigue-resistant, oxidative (SO) fibers, (2) fast-twitch, oxidative-glycolytic (FOG) fibers, and (3) fast-twitch, glycolytic, fatigueable (FG) fibers. These fiber types are established during development, and in adults, they display a remarkable adaptation to functional and metabolic demands, responding by a fiber-type switching to altered workload and frequency of motor nerve stimulation (Berchtold et al. [2000]; Fluck and Hoppeler [2003], and references therein). Moreover, caloric restriction retards age-related slow-to-fast fiber-type conversion in rats (Aspnes et al., 1997), and studies of humans and rodents have indicated a correlation between (1) obesity and/or diabetes and (2) reduced muscle oxidative capacity and/or fiber type composition. However, it is not known whether replacement of oxidative fibers by glycolytic fibers is a cause or a consequence of obesity or diabetes (Patti et al. [2003], Petersen et al. [2003], Tanner et al. [2002], Wisloff et al. [2005], and references therein).

Peroxisome proliferator-activated receptors (PPARs) are members of the nuclear receptor superfamily that form heterodimers with retinoid X receptors (RXRs) and bind preferentially to direct repeats of the consensus hexameric nucleotide sequence 5′-AGGTCA-3′ separated by 1 base (DR1), called peroxisome proliferator-activated receptor response elements (PPREs), to control target gene expression. Three PPAR isotypes (α, β, and γ), with distinct tissue distribution, have been identified. PPARα (NR1C1) is preferentially expressed in tissues with high fatty acid (FA) oxidation, such as heart, kidney, brown adipose tissue (BAT), and liver, where it regulates FA transport, esterification and oxidation via transcriptional activation of genes encoding enzymes involved in each step of FA breakdown. PPARγ (NR1C3) is predominant in adipose tissue and plays an essential role in adipocyte differentiation and survival (Desvergne and Wahli, 1999; Evans et al., 2004; Metzger et al., 2005). In contrast, PPARβ (δ; NR1C2), which is expressed ubiquitously, is the most abundant PPAR isotype in skeletal muscle (Escher et al., 2001). Increases of PPARβ activity through ligand activation, PPARβ overexpression, or expression of a constitutively active PPARβ in transgenic mice, have recently suggested that this receptor could be physiologically involved in fatty acid metabolism and muscle fiber-type switching (Evans et al., 2004). To investigate whether PPARβ is actually a key player in these processes, we have generated PPARβ$^{skm-/-}$ mice, in which PPARβ is selectively ablated in skeletal muscle myocytes. We show that these mice exhibit a functional switch of the skeletal muscle fiber type toward lower oxidative capacity that precedes the appearance of age-dependent obesity and type 2 diabetes.

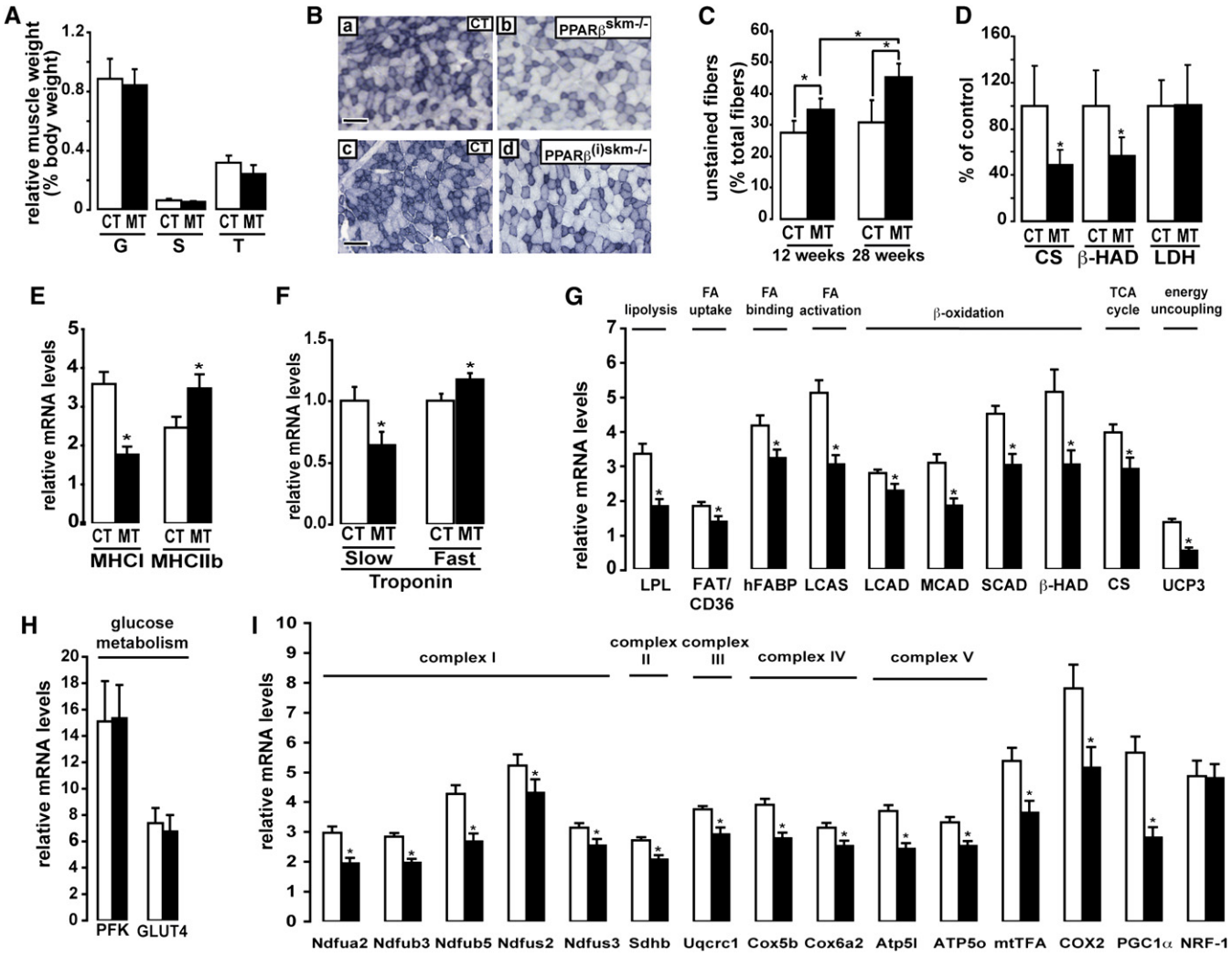

Figure 1. Characterization of PPARβ-deficient skeletal muscles

A) Relative weight of fast (G, gastrocnemius), slow (S, soleus) and mixed (T, tibialis) muscles from 28 week-old CT and MT mice (n = 6–8).

B) Histochemical NADH-tetrazolium reductase staining of tibialis muscles of 28 week-old CT (a) and PPARβ$^{skm-/-}$ (b) mice, and 20 week-old CT (c) and PPARβ$^{(i)skm-/-}$ (d) mice. Three different fiber types are distinguished: oxidative (SO) and intermediate (FOG) fibers are darkly and moderately stained, respectively; glycolytic fibers (FG) are unstained. Scale bar, 100 μm.

C) Percentage of unstained fibers in tibialis muscles of 12 and 28 week-old CT and MT mice (n = 4–6).

D) Biochemical determination of CS, β-HAD, and LDH activities in tibialis extracts of 12 week-old CT and PPARβ$^{skm-/-}$ (MT) mice (n = 4).

E) Relative MHCI and MHCIIb transcript levels in gastrocnemius muscle of 16 week-old CT and MT mice.

F) Relative troponin I slow and fast transcript levels in gastrocnemius muscle of 16 week-old CT and MT mice.

G) Relative transcript levels in gastrocnemius muscle of 10–12 week-old CT and MT mice of genes involved in FA metabolism and energy uncoupling (UCP 3). LPL, lipoprotein lipase; FAT/CD36, fatty acid translocase; hFABP, heart fatty-acid binding protein; LCAS, long chain acyl-CoA synthetase; LCAD, MCAD, and SCAD, long-, medium-, and short-chain acyl-CoA dehydrogenase; β-HAD, β-hydroxy-acyl-CoA dehydrogenase; CS, citrate synthase.

H) Relative transcript levels of genes involved in glucose metabolism. PFK, phosphofructokinase 1; GLUT4, glucose transporter 4.

I) Relative transcript levels of genes of the mitochondrial electron transport chain and of transcription factors controlling their expression, as indicated (n = 7–11).

We also demonstrate that the expression of PGC1α, a transcriptional coregulator that coordinates the formation/maintenance of slow fibers in skeletal myocytes, is directly controlled by PPARβ.

Results

To selectively ablate PPARβ in skeletal muscle, PPARβ$^{L2/L2}$ mice bearing floxed PPARβ L2 alleles (in which LoxP sites flank the PPARβ exon encoding the N-terminal zinc finger of the DNA binding domain) were bred with HSA-Cre$^{tg/0}$ mice that express the Cre recombinase under the control of the human α-skeletal actin promoter (Miniou et al., 1999) to produce control mice (CT) as well as HSA-Cre$^{tg/0}$/PPARβ$^{L2/L2}$ somatic mutants (MT) in which PPARβ is selectively ablated in skeletal muscles (PPARβ$^{skm-/-}$ mice; Supplemental Data).

Muscle-to-body weight ratios and the morphology of gastrocnemius (G), soleus (S), and tibialis (T) muscles were similar in 12 and 28 week-old CT and MT (Figure 1A and data not shown). However, histochemical staining with NADH-tetrazolium reductase, a marker of the mitochondrial respiratory chain complex I activity, revealed a 40% increase of unstained FG in tibialis

muscles of 12 week-old MT mice (MT, 35%; CT, 25%), and a corresponding lower number of stained fibers (FOG and SO; Figure 1B, panels a and b), indicating that muscle fibers in MT were less oxidative than in CT. In 28 week-old MT, the percentage of NADH-tetrazolium reductase unstained fibers was further increased to reach 45%, whereas it was unchanged in CT (Figure 1C), showing an age-dependent decrease of oxidative capacity in PPARβ-deficient skeletal muscles. Interestingly, selective ablation of PPARβ in skeletal muscles of adult mice [PPARβ$^{(i)skm-/-}$ mice], induced by Tamoxifen administration to PPARβ$^{L2/L2}$ mice bearing the HSA-Cre-ER^{T2} transgene (Schuler et al., 2005), also resulted in a lower oxidative capacity of skeletal muscle (Figure 1B, compare panels c and d).

To further characterize muscle oxidative capability, enzyme activities of the aerobic oxidative pathways (fatty acid oxidation and tricarboxylic acid cycle [TCA]) and of the glycolytic pathways were analyzed in tibialis muscle extracts of 12 week-old mice. The activity of β-hydroxy-acyl-CoA dehydrogenase (β-HAD, aerobic-oxidative pathway, FA oxidation) and citrate synthase (CS, aerobic-oxidative pathway, TCA) were 50% lower in MT than CT, whereas the activity of the glycolytic enzyme lactate dehydrogenase (LDH) was unchanged (Figure 1D; data not shown). To determine the fiber-type composition, the expression of myosin heavy chain (MHC) isoforms was analyzed in gastrocnemius of 16 week-old mice by quantitative RT-PCR. The transcript levels of the slow MHCI was ~50% lower in MT than in CT, whereas those of fast MHCIIb were ~25% higher in MT (Figure 1E). Moreover, Troponin I slow RNA levels were reduced by ~35% in MT, whereas those of troponin I fast were increased by ~20% in MT (Figure 1F).

Quantitative RT-PCR analysis of 10–12 week-old mouse gastrocnemius muscle revealed that transcript levels of genes controlling (1) lipolysis (LPL); (2) FA uptake (FAT/CD36), binding (hFABP), activation (LCAS), and β-oxidation (LCAD, MCAD, SCAD, β-HAD); and (3) the TCA cycle (CS) were 20%–40% lower in MT. Moreover, the transcript level of uncoupling protein (UCP) 3, a putative target of PPARβ-specific ligands in skeletal muscle cells (Muoio et al., 2002), was 50% lower in MT (Figure 1G), whereas those of two genes of the glycolytic pathway (PFK and GLUT4) were similar in CT and MT (Figure 1H).

As the histochemically determined mitochondrial respiratory chain complex I activity was lower in MT than in CT (Figures 1B and 1C), we also analyzed the transcript levels of nuclear genes encoding components of the respiratory chain. The transcripts of Ndfua2, Ndfub3, Ndfub5, Ndfus2, and Ndfus3 (complex I); Sdhb (complex II); Uqcrc1 (complex III); Cox5b and Cox6a2 (complex IV); as well as Atp5l and Atp5o (complex V) were 20%–40% lower in MT. Moreover, the transcript level of the mitochondrial transcription factor A (mtTFA), which regulates transcription of mitochondrial genes encoding respiratory chain proteins, was 20% lower in the MT gastrocnemius muscles, and the RNA level of the mitochondrial Cox 2 gene was reduced by about 20% in MT (Figure 1I). Interestingly, the transcript level of PGC1α, which binds and coactivates the transcriptional function of nuclear respiratory factor-1 (NRF-1) on the mtTFA promoter (Wu et al., 1999), was 2-fold lower in MT than in CT (Figure 1I), whereas those of NRF-1 were unchanged. Gastrocnemius mitochondrial DNA content was however similar in CT and MT at 8 and 26 weeks (data not shown). Note that transcript levels of UCP1, 2, and 3 and PPARα in BAT; those of leptin, FAS, SREBP-1, and PPARγ in white adipose tissue (WAT); and those of MCAD and PPARα in liver were similar in CT and MT (data not shown). Taken together, these data show that the transcript levels of many genes involved in FA metabolism, as well as of a number of nuclear and mitochondrial genes encoding components of the mitochondrial electron transport chain, were selectively reduced in PPARβ$^{skm-/-}$ mouse skeletal muscles whose fibers were shifted toward a more fast-twitch, glycolytic type.

As skeletal muscle oxidative capacity decreased with time in PPARβ$^{skm-/-}$ mice, we subjected 43 week-old mice to endurance exercise performance tests. The treadmill running time and distance until exhaustion was ~30% lower in PPARβ$^{skm-/-}$ than in CT (Figure S2). These reductions in MT were not due to greater body weight of MT, as similar variations in endurance performance tests were observed with weight-matched CT and MT (data not shown). In contrast, spontaneous locomotor activity (determined with an open field test) was similar in CT and MT (data not shown). Thus, the lower number of slow oxidative fibers in MT resulted in markedly reduced capacity to sustain running exercise.

The decrease in PGC1α transcripts in PPARβ$^{skm-/-}$ muscles prompted us to investigate whether PPARβ might directly control PGC1α expression. Sequence analysis of the PGC1α promoter revealed a conserved putative PPRE (5′-AGGACA A AGGTCA-3′), located between nucleotides 2024 and 2043 and between nucleotides 1872 and 1891, upstream of the mouse (m) and human (h) PGC1α transcriptional initiation site, respectively (Figure 2A). Electrophoretic mobility shift assays showed that PPARβ/RXRα heterodimers efficiently bound the PGC1α PPRE; no binding could be observed when it was mutated in its 3′ and 5′ repeated motifs (PGC1α PPREm; Figure 2B, compare lanes 1 and 2), and PPARβ/RXRα binding to PGC1α PPRE was efficiently competed out with an excess of unlabeled wild-type PPRE but not with PGC1α PPREm (Figure 2B; lanes 3–6 and 7–10). Moreover, treatment of C2C12 myocytes with the PPARβ-selective agonist GW501516 (Oliver et al., 2001) and the RXR selective agonist BMS649 (Roy et al., 1995) induced PGC1α transcripts by 4-fold (Figure 2C). To support the possibility that PPARβ could control the activity of PGC1α promoter in muscle cells, C2C12 myoblasts were transiently transfected with a luciferase reporter gene (pGL-PGC1α) driven by a 4 kb mouse PGC1α promoter/enhancer region and differentiated into myocytes. Addition of the PPARβ-specific agonist GW501516 stimulated luciferase activity 2-fold, and this ligand-dependent stimulation of PGC1α promoter activity was abolished when its PPRE was mutated (pGL-PGC1αm; Figure 2D). In contrast, the PPARγ-selective ligand rosiglitazone stimulated the PGC1α promoter activity only 1.2-fold, and the PPARα-selective ligand WY14643 had no effect (Figure 2D). Thus, PGC1α promoter activity can be enhanced by liganded PPARβ in muscle cells via a PPRE located between nucleotides 2024 and 2043 upstream of the mouse PGC1α start site.

Food intake and basal metabolic rate were similar in CT and MT (data not shown). However, PPARβ$^{skm-/-}$ mice fed a regular diet gained more weight than CT (Figures 3A and 3B; data not shown); 28 week-old PPARβ$^{skm-/-}$ mice were 5.5 g heavier than CT mice. This difference was not due to increased muscle weight (Figure 1A), but to increased body fat content and WAT weight (Figures 3C and 3D). Histological analysis of epididymal fat pad revealed that adipocytes were hypertrophic in 28 week-old obese PPARβ$^{skm-/-}$ mice (Figure 3E), indicating that

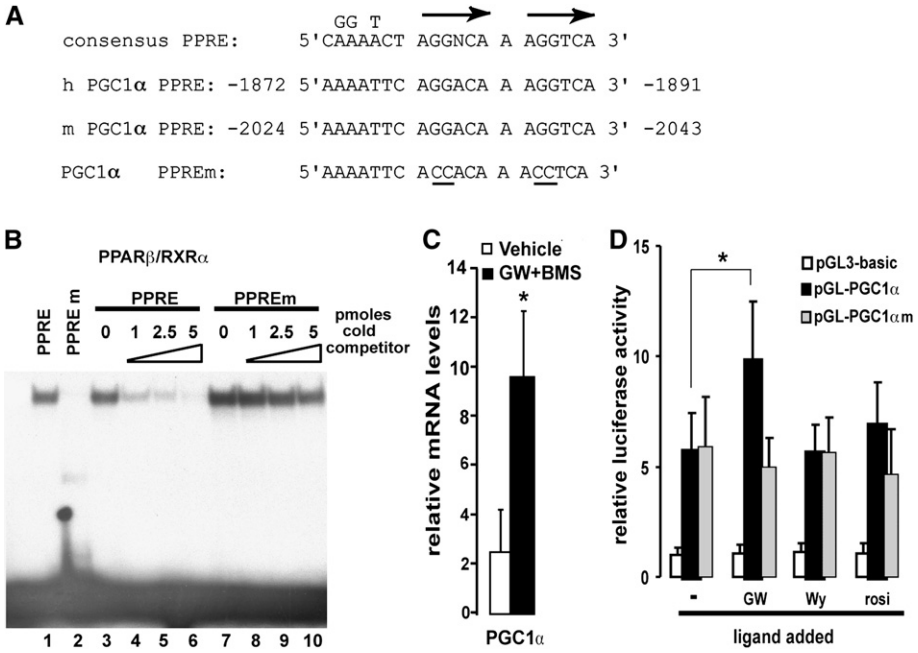

Figure 2. Functional characterization of the PGC1α-PPRE

A) Sequence of the consensus, wild-type human and mouse, and mutated PGC1α-PPRE.

B) Electrophoretic mobility shift assay (EMSA) of radiolabeled PGC1α PPRE using PPARβ and RXRα. In vitro synthesized nuclear receptors were incubated with the wild-type (lanes 1 and 3–10) and mutant (lane 2) PGC1α PPRE (PGC1α PPREm), in the absence (lanes 1–3 and 7) or presence of increasing concentrations of unlabeled PGC1α PPRE (lane 4–6) or PGC1α PPREm (lane 8–10).

C) Relative PGC1α transcript levels in C2C12 myocytes treated with vehicle or GW501516 and BMS649 (GW + BMS) (n = 3).

D) Luciferase activity was determined on C2C12 myoblast transfected with pGL3-basic, pGL-PGC1α, or pGL-PGC1αm luciferase reporter vectors, and grown in the absence or presence of GW501516 (GW), WY14643 (WY), or rosiglitazone (rosi). Data are expressed as mean values ± SEM, relative to vehicle-treated pGL3-transfected cells.

impaired muscular FA breakdown in PPARβ$^{skm-/-}$ animals leads to increased fatty acid storage in adipose tissue. Serum glucose, insulin, and triglyceride levels after a 6 hr fast were 1.2-, 1.8-, and 1.4-fold higher in 12 week-old MT than in CT mice, respectively (Figure 4A), and circulating nonesterified free fatty acid levels were slightly increased in MT (1.1-fold, which did not reach statistical significance; data not shown). Moreover, insulin efficiently decreased glucose levels in these mice when subjected to an intraperitoneal insulin tolerance test (Figure 4B). However, 8 month-old MT mice were insulin-resistant and glucose-intolerant (Figures 4C and 4D), indicating that mice lacking PPARβ in skeletal muscles develop an age-dependent type 2 diabetes. Interestingly, serum levels of the adipokine adiponectin were 20% lower in aged MT than in aged CT, whereas those of leptin were similar (data not shown).

Upon an 8 week high fat diet (HFD) treatment that started at 5 weeks of age, the MT body weight was 35% higher in MT than CT (Figure 3B). Moreover, after 8 weeks of HFD feeding, TG serum levels were 25% higher in MT than in CT (Figure 3F), and MT were more insulin-resistant than CT when subjected to an intraperitoneal insulin tolerance test (Figure 3G).

Discussion

Previous studies have suggested that PPARβ could control skeletal muscle oxidative capacity and slow fiber-type formation in mice (Luquet et al., 2003; Tanaka et al., 2003; Wang et al., 2004). We show here that Cre recombinase-mediated selective ablation of PPARβ in skeletal muscle myocytes results in an age-dependent reduction of muscle oxidative capacity and induces a functional muscle fiber-type switching toward less oxidative fibers. Importantly, the fiber-type switching precedes obesity and diabetes and appears to be the cause and not the consequence of these metabolic disorders. Indeed, even though glucose homeostasis is impaired at an early time, only aged MT mice are insulin resistant. Interestingly, serum adiponectin levels, known to be decreased in insulin-resistant states (Kadowaki et al., 2006), were also decreased in aged MT mice. Thus, whole-body insulin resistance might appear when a critical fraction of the SO fibers have been converted to FG fibers and/or after reaching a ''given stage'' of obesity, when the levels of adipokines known to play an important role in whole body insulin sensitivity, are ''altered'' (Lazar, 2005). A similar decrease in muscle oxidative capacity was obtained by PPARβ ablation in skeletal myocytes of adult mice, using transgenic mice expressing the tamoxifen-dependent Cre-ER^{T2} recombinase under the skeletal actin promoter (Schuler et al., 2005), thus demonstrating that PPARβ is instrumental in myocytes for the maintenance of their oxidative capacity.

Exercise training is known to increase PPARβ levels in skeletal muscles (Luquet et al., 2003), and PPARβ levels are higher in slow-twitch oxidative than in fast-twitch glycolytic muscles in mice (Wang et al., 2004). Our data therefore point to a mechanism whereby increased levels of PPARβ could be instrumental in muscle fiber-type switch. PGC1α is known to play an important role in the formation/maintenance of slow muscle fibers (Leone et al., 2005; Lin et al., 2005). PGC1α levels are higher in slow-twitch oxidative than in fast-twitch glycolytic muscles in mice, and exercise training increases muscle PGC1α levels via a calcium signaling cascade, including calcineurin, calmodulin dependent kinase IV (CaMKIV), myocyte enhancer factor 2 (MEF2), CREB, and nuclear factor of activated T cells (NFAT) (Lin et al., 2005; see Figure 4E). Importantly, we found in the mouse and human PGC1α promoter/enhancer region a conserved PPRE that specifically binds PPARβ/RXRα heterodimers in vitro. Moreover, the PPARβ-selective agonist GW 501516 stimulates the activity of the mouse PGC1α promoter through this PPRE in C2C12 myocytes. In keeping with these findings, PGC1α transcript levels are reduced in skeletal muscles of PPARβ$^{skm-/-}$ mouse mutants (Figure 1I), and PPARβ-selective ligands enhance PGC1α transcript levels in mouse skeletal muscles (Figure 2D; Tanaka et al., 2003). It appears therefore that

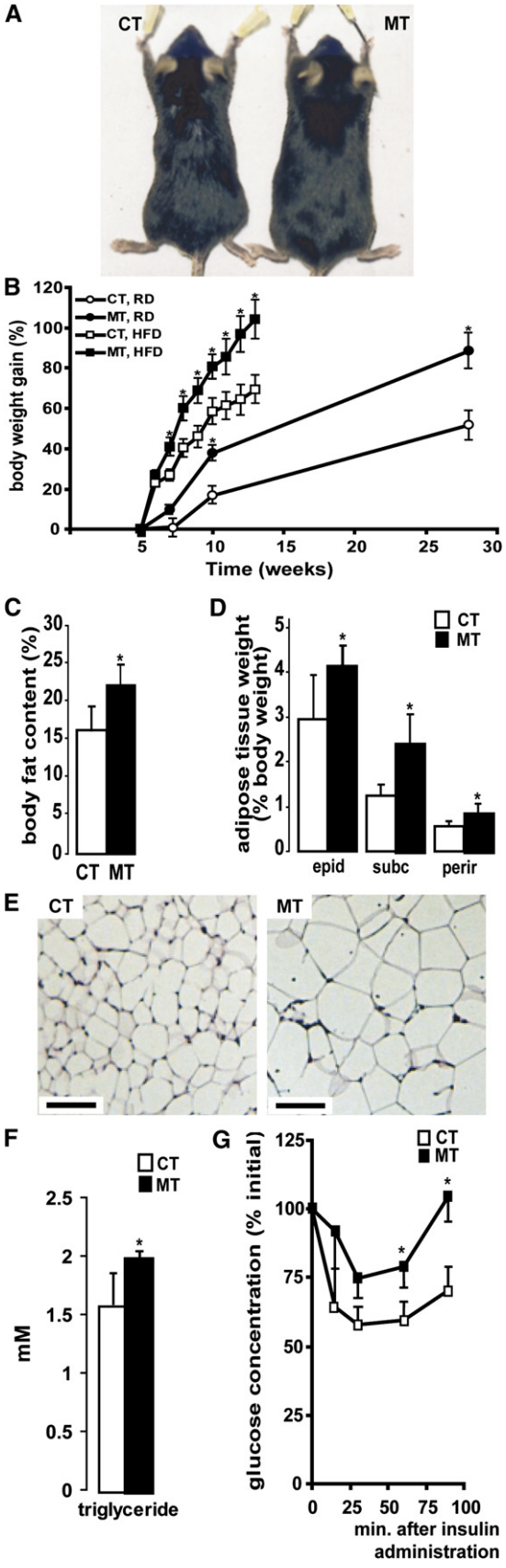

liganded PPARβ participates in the formation/maintenance of slow muscle fiber type by stimulating PGC1α expression in muscle cells (Figure 4E). However, it has been reported that PGC1α levels are inversely correlated with intramuscular fatty acid levels in rodents (Benton et al. [2006] and references therein) and also that unsaturated but not saturated fatty-acids increased PGC1α expression in differentiated myotubes (Staiger et al., 2005). This suggests that in skeletal muscles the ligands that activate PPARβ are selected fatty acids or fatty-acid metabolites.

Interestingly, as PGC1α is known to act as a PPARβ coactivator (Dressel et al., 2003; Wang et al., 2003), the PGC1α promoter activity can be enhanced through a feed-forward loop similar to that resulting from the interaction of PGC1α with MEF2 (Handschin et al., 2003), another transcriptional activator that binds to the PGC1α promoter. Together, these two feed-forward loops may ensure a stable transcription of PGC1α, leading to efficient maintenance of slow fatigue-resistant muscle fibers, as well as to sustained increase in muscle mitochondrial oxidation capacity (Figure 4E). In this respect, we note that a recent report (Hondares et al., 2006) has shown that the PGC1α gene is a direct target of PPARγ in brown and white adipocytes, which suggests that PGC1α expression could be differentially regulated in adipocytes and myocytes.

In summary, our data demonstrate that PPARβ is required in skeletal muscles for the maintenance of slow oxidative fibers, and that this effect is mediated, at least in part, through the control of expression of PGC1α at the transcriptional level. Furthermore, we have established that ablation of PPARβ in mouse skeletal muscles leads to obesity and diabetes. As physical exercise is known to result in a PPARβ increase in skeletal muscles, its beneficial effects in preventing obesity and diabetes could be mediated, at least in part, through induction of PPARβ signaling at the level of the receptor and/or its cognate ligand(s). Whether this induction is triggered by muscle contraction through the calcium signaling cascade, as in the case of PGC1α, remains to be investigated (Figure 4E).

Experimental procedures

Mice

Mice were maintained in a temperature- and humidity-controlled animal facility, with a 12 hr light/dark cycle and free access to water and a standard rodent chow (2800 kcal/kg, Usine d'Alimentation Rationelle, Villemoisson-sur-Orge, France). The HFD study was carried out with a chow containing 4,056 kcal/kg (fat: 1,600 kcal/kg and sucrose: 1,600 kcal/kg; research Diets, New Brunswick, New Jersey). HFD was given to mice at weaning. Body weight

Figure 3. Increased adiposity in aging PPARβ$^{skm-/-}$ animals

A) Dorsal view of a 25 week-old regular diet fed CT and PPARβ$^{skm-/-}$ mouse.

B) Body weight gain of CT and PPARβ$^{skm-/-}$ mice fed a regular (RD) or high fat (HFD) diet (n = 6–10) (RD cohorte: body weight at week 5: CT, 24 ± 1.8 g; MT, 22.3 ± 1.0 g; body weight gain between week 5 and 28: CT, 52%; MT, 88%; HFD cohorte: HFD: body weight at week 5; CT, 19, 3 ± 1.15 g; MT, 18.5 ± 1.87 g, p = 0, 37; body weight gain between week 5 and 13: CT, 70%; MT, 105%).

C) Total body fat content in 17 week-old RD-fed CT and MT mice determined by DEXA (n = 6–10).

D) Relative epididymal, subcutaneous, and perirenal WAT weight of 28 week-old RD-fed CT and MT mice.

E) Histology of epididymal WAT of 28 week-old RD-fed CT and MT mice. Scale bar, 160 μm.

F) Serum triglyceride levels in 13 week-old HFD-fed CT and MT mice (n = 5).

G) Intraperitoneal insulin tolerance test in 13 week-old HFD-fed CT and MT mice (n = 4–6).

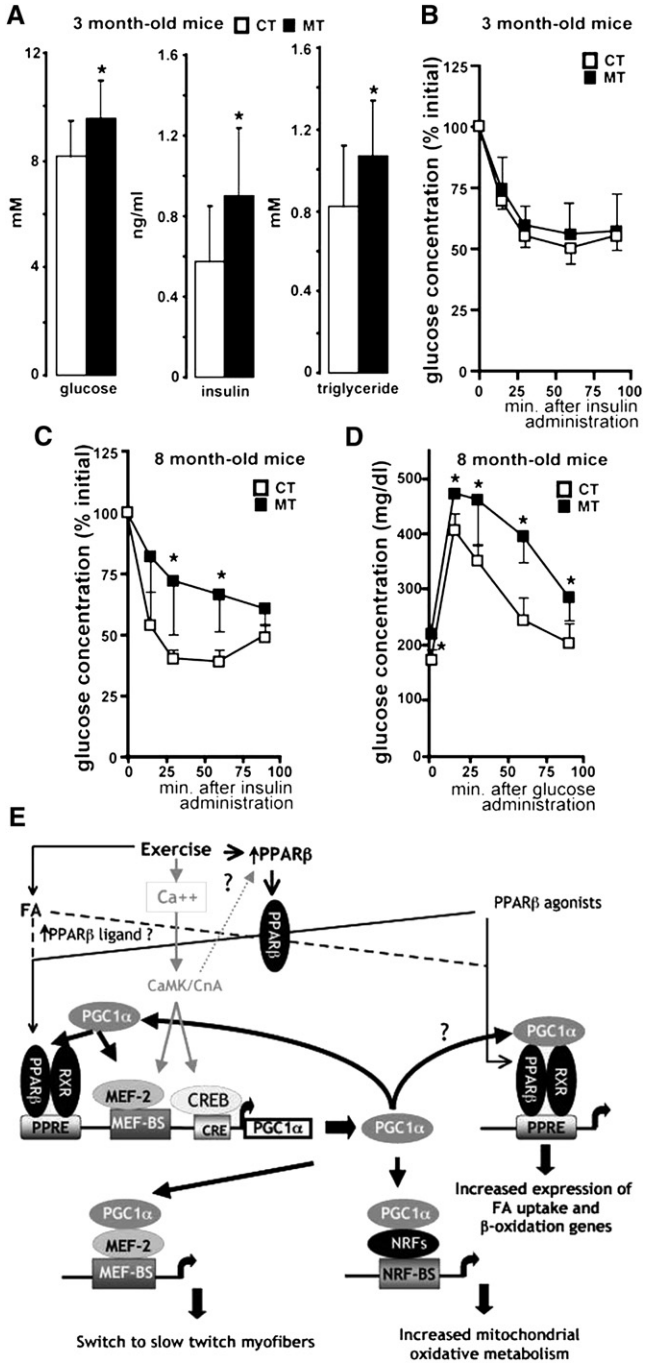

Figure 4. Impaired glucose homeostasis in PPARβ$^{skm-/-}$ mice and schematic model of exercice-induced fiber type switching

A) Serum glucose, insulin and triglyceride levels in 12 week-old CT and MT mice (n > 8).

B–D) Intraperitoneal insulin **(B and C)** and **(D)** glucose tolerance tests in 12 **(B)** and 32 **(C and D)** week-old mice (n = 4–6).

E) Schematic model of exercice-induced fiber-type switching. The PGC1α promoter/enhancer region contains a PPRE, a MEF binding site (MEF-BS), and a cAMP response element (CRE). Muscle contraction induces a calcium-signaling pathway that activates CREB and MEF2 via CamKIV and calcineurinA (CnA) and thus stimulates PGC1α promoter activity. Exercise increases PPARβ levels (through an unknown mechanism) and may also increase the level of PPARβ ligands (fatty acids, FA). Increased PPARβ activity further enhances PGC1α expression. Moreover, PGC1α by coactivating MEF2 and PPARβ provides a positive feed-forward signal to further increase PGC1α expression. In turn, PGC1α stimulates the expression of NRF1 and NRF2, thus leading to enhanced expression of nuclear-encoded mitochondrial genes. PGC1α simultaneously regulates the switch to slow-twitch muscle fiber genes through coactivation of MEF2. PPARβ/RXR heterodimers also stimulate the expression of genes involved in fatty acid uptake and β-oxidation, and PGC1α may potentiate it.

was determined at the indicated ages, and body-fat content was evaluated in anaesthetized mice by dual X-ray absorptiometry (DEXA; PIXIMUS, GE Medical Systems, Buc, France). Blood was collected from the retroorbital sinus after a 6 hr fast that started at the beginning of the light cycle, and serum glucose, insulin, and triglycerides levels were analyzed as described (Picard et al., 2002). Insulin and glucose tolerance tests were performed on 3 and 8–9 month-old mice that were fasted for 3 hr. Glucose concentrations were determined with a OneTouch® blood glucometer (LifeScan, Lissy les Moulineaux, France) in blood collected from the tail vein before (0 min) and 15, 30, 60, and 90 min after intraperitoneal injection of insulin (1 U/kg, bovine insulin from Sigma) or glucose (2g/kg).

Animals were killed by CO_2 inhalation at the beginning of the light cycle, and tissues were collected, weighed, and frozen in liquid nitrogen or processed for biochemical and histological analysis.

Histological and histochemical analysis

Muscles were quickly frozen in dry ice-cooled isopentane. For NADH-tetrazolium reductase staining, 10 μm cryosections were incubated in 0.2 M Tris, pH 7.4, containing 1.5 mM NADH and 1.5 mM nitrobluetetrazolium for 15 min at 55°C, dehydrated, and mounted. SO and FOG fibers are positively stained, whereas FG fibers remain unstained (Hamalainen and Pette, 1993). Epididymal WAT was fixed in Bouin's solution, dehydrated in ethanol, embedded in paraffin, and cut at a thickness of 10 μm. Sections were deparaffinized, rehydrated, and stained with haematoxylin and eosin.

Electrophoretic mobility shift assays

pSG5-based PPARβ and RXRα expression plasmids were in vitro transcribed/translated using the TnT® Quick coupled transcription/translation system according to the manufacturer's recommendations (Promega). EMSAs were performed as described (Rochette-Egly et al., 1994), using 0.05 pmol of end-labeled oligonucleotide pairs. The PGC1α-PPRE and the PGC1α-PPREm were obtained by annealing oligonucleotides 5′-GATC CAAAATTCAGGACAAAGGTCAG-3′ and 5′-GATCCTGACCCTTTGTTCCC CTGAATTTTG-3′, and 5′-AGCCCATGAGGTTTGTGGTGAATTTTAATA-3′ and 5′-TATTAAAATTCACCACAAACCTCATGGGCT-3′, respectively. Unlabeled oligonucleotide pairs were added to the binding reaction for competition experiments.

Cell culture and transfection assays

5.10^4 C2C12 myoblasts were seeded in 24-well plates and grown for 24 hr in proliferation medium (Dulbecco's modified Eagle medium [DMEM]; glucose, 1 g/l, supplemented with 20% delipidated FCS). 0.2 μg pCMV-βgal and 0.8 μg pGL-PGC1α, pGL-PGC1αm or pGL3-basic (see Supplemental Data) was mixed with 3 μl of Fugene6 transfection reagent (Roche Diagnostics) in 100 μl DMEM, according to the supplier's protocol. After 15 min at room temperature, 30 μl transfection mix was added to each well, and the medium was changed 7 hr later to differentiation medium (DMEM supplemented with 5% delipidated FCS), containing the PPARα ligand Wy 14643 (10 μM), the PPARβ ligand GW501516 (1 μM), or the PPARγ ligand rosiglitazone (50 μM). Sixteen hours later, cells were harvested, lysed, and assayed for β-galactosidase (Voegel et al., 1998) and luciferase activity (Promega). Each transfection was done in triplicate. Luciferase activity was normalized to the β-galactosidase activity, and data are expressed as fold difference relative to the normalized luciferase activity of pGL3-basic transfection in the absence ligand, which was set as 1.

For RNA preparation, 3.10^5 C2C12 myoblasts were seeded in 6-well plates and grown for 30 hr in proliferation medium supplemented with 20% delipidated FCS. The medium was changed 30 hr later to differentiation medium, containing 1 μM GW501516 and 10 μM BMS961 or vehicle, and cells were harvested 16 hr later.

Data analysis

Data are presented as mean ± SEM. Differences analyzed by a two-tailed Student's t test were considered statistically significant at $p < 0.05$ and are indicated by an asterisk in the figures.

Supplemental data

Supplemental Data include Supplemental Results, Supplemental Experimental Procedures, and two figures and can be found with this article online at http://www.cellmetabolism.org/cgi/content/full/4/5/407/DC1/.

Acknowledgments

We thank Dr. J. Melki for HSA-Cre mice, the staff of the mouse, histopathology and biochemistry of the ICS and IGBMC for technical assistance, J. Auwerx for helpful discussions, and the secretarial staff for preparation of the manuscript. This work was supported by funds from the Centre National de la Recherche Scientifique, the Institut National de la Santé et de la Recherche Médicale, the Collège de France, the Association pour la Recherche sur le cancer, the Fondation pour la Recherche Médicale, the Human Frontier Science Program, the Ministère de l'Education Nationale, de la Recherche et de la Technologie, the Swiss National Science Foundation, the Etat de Vaud, and the European Community. M.S. was supported by a Marie Curie Individual fellowship and an ARI fellowship, C.C. by an ARI fellowship, and F.A. by a Boehringer Ingelheim Fund fellowship.

Received: January 24, 2006
Revised: August 20, 2006
Accepted: October 3, 2006
Published: November 7, 2006

References

Aspnes, L.E., Lee, C.M., Weindruch, R., Chung, S.S., Roecker, E.B., and Aiken, J.M. (1997). Caloric restriction reduces fiber loss and mitochondrial abnormalities in aged rat muscle. FASEB J. *11*, 573–581.

Benton, C.R., Han, X.X., Febbraio, M., Graham, T.E., and Bonen, A. (2006). Inverse relationship between PGC-1alpha protein expression and triacylglycerol accumulation in rodent skeletal muscle. J. Appl. Physiol. *100*, 377–383.

Berchtold, M.W., Brinkmeier, H., and Muntener, M. (2000). Calcium ion in skeletal muscle: its crucial role for muscle function, plasticity, and disease. Physiol. Rev. *80*, 1215–1265.

Desvergne, B., and Wahli, W. (1999). Peroxisome proliferator-activated receptors: nuclear control of metabolism. Endocr. Rev. *20*, 649–688.

Dressel, U., Allen, T.L., Pippal, J.B., Rohde, P.R., Lau, P., and Muscat, G.E. (2003). The peroxisome proliferator-activated receptor beta/delta agonist, GW501516, regulates the expression of genes involved in lipid catabolism and energy uncoupling in skeletal muscle cells. Mol. Endocrinol. *17*, 2477–2493.

Escher, P., Braissant, O., Basu-Modak, S., Michalik, L., Wahli, W., and Desvergne, B. (2001). Rat PPARs: quantitative analysis in adult rat tissues and regulation in fasting and refeeding. Endocrinology *142*, 4195–4202.

Evans, R.M., Barish, G.D., and Wang, Y.X. (2004). PPARs and the complex journey to obesity. Nat. Med. *10*, 355–361.

Fluck, M., and Hoppeler, H. (2003). Molecular basis of skeletal muscle plasticity–from gene to form and function. Rev. Physiol. Biochem. Pharmacol. *146*, 159–216.

Hamalainen, N., and Pette, D. (1993). The histochemical profiles of fast fiber types IIB, IID, and IIA in skeletal muscles of mouse, rat, and rabbit. J. Histochem. Cytochem. *41*, 733–743.

Handschin, C., Rhee, J., Lin, J., Tarr, P.T., and Spiegelman, B.M. (2003). An autoregulatory loop controls peroxisome proliferator-activated receptor gamma coactivator 1alpha expression in muscle. Proc. Natl. Acad. Sci. USA *100*, 7111–7116.

Hondares, E., Mora, O., Yubero, P., de la Concepcion, M.R., Iglesias, R., Giralt, M., and Villarroya, F. (2006). Thiazolidinediones and rexinoids induce peroxisome proliferator-activated receptor-coactivator (PGC)-1alpha gene transcription: an autoregulatory loop controls PGC-1alpha expression in adipocytes via peroxisome proliferator-activated receptor-gamma coactivation. Endocrinology *147*, 2829–2838.

Kadowaki, T., Yamauchi, T., Kubota, N., Hara, K., Ueki, K., and Tobe, K. (2006). Adiponectin and adiponectin receptors in insulin resistance, diabetes, and the metabolic syndrome. J. Clin. Invest. *116*, 1784–1792.

Lazar, M.A. (2005). How obesity causes diabetes: not a tall tale. Science *307*, 373–375.

Leone, T.C., Lehman, J.J., Finck, B.N., Schaeffer, P.J., Wende, A.R., Boudina, S., Courtois, M., Wozniak, D.F., Sambandam, N., Bernal-Mizrachi, C., et al. (2005). PGC-1alpha deficiency causes multi-system energy metabolic derangements: muscle dysfunction, abnormal weight control and hepatic steatosis. PLoS Biol. *3*, e101.

Lin, J., Handschin, C., and Spiegelman, B.M. (2005). Metabolic control through the PGC-1 family of transcription coactivators. Cell Metab. *1*, 361–370.

Luquet, S., Lopez-Soriano, J., Holst, D., Fredenrich, A., Melki, J., Rassoulzadegan, M., and Grimaldi, P.A. (2003). Peroxisome proliferator-activated receptor delta controls muscle development and oxidative capability. FASEB J. *17*, 2299–2301.

Metzger, D., Imai, T., Jiang, M., Takukawa, R., Desvergne, B., Wahli, W., and Chambon, P. (2005). Functional role of RXRs and PPARgamma in mature adipocytes. Prostaglandins Leukot. Essent. Fatty Acids *73*, 51–58.

Miniou, P., Tiziano, D., Frugier, T., Roblot, N., Le Meur, M., and Melki, J. (1999). Gene targeting restricted to mouse striated muscle lineage. Nucleic Acids Res. *27*, e27.

Muoio, D.M., MacLean, P.S., Lang, D.B., Li, S., Houmard, J.A., Way, J.M., Winegar, D.A., Corton, J.C., Dohm, G.L., and Kraus, W.E. (2002). Fatty acid homeostasis and induction of lipid regulatory genes in skeletal muscles of peroxisome proliferator-activated receptor (PPAR) alpha knock-out mice. Evidence for compensatory regulation by PPAR delta. J. Biol. Chem. *277*, 26089–26097.

Oliver, W.R., Jr., Shenk, J.L., Snaith, M.R., Russell, C.S., Plunket, K.D., Bodkin, N.L., Lewis, M.C., Winegar, D.A., Sznaidman, M.L., Lambert, M.H., et al. (2001). A selective peroxisome proliferator-activated receptor delta agonist promotes reverse cholesterol transport. Proc. Natl. Acad. Sci. USA *98*, 5306–5311.

Patti, M.E., Butte, A.J., Crunkhorn, S., Cusi, K., Berria, R., Kashyap, S., Miyazaki, Y., Kohane, I., Costello, M., Saccone, R., et al. (2003). Coordinated reduction of genes of oxidative metabolism in humans with insulin resistance and diabetes: Potential role of PGC1 and NRF1. Proc. Natl. Acad. Sci. USA *100*, 8466–8471.

Petersen, K.F., Befroy, D., Dufour, S., Dziura, J., Ariyan, C., Rothman, D.L., DiPietro, L., Cline, G.W., and Shulman, G.I. (2003). Mitochondrial dysfunction in the elderly: possible role in insulin resistance. Science *300*, 1140–1142.

Picard, F., Gehin, M., Annicotte, J., Rocchi, S., Champy, M.F., O'Malley, B.W., Chambon, P., and Auwerx, J. (2002). SRC-1 and TIF2 control energy balance between white and brown adipose tissues. Cell *111*, 931–941.

Rochette-Egly, C., Lutz, Y., Pfister, V., Heyberger, S., Scheuer, I., Chambon, P., and Gaub, M.P. (1994). Detection of retinoid X receptors using specific monoclonal and polyclonal antibodies. Biochem. Biophys. Res. Commun. *204*, 525–536.

Roy, B., Taneja, R., and Chambon, P. (1995). Synergistic activation of retinoic acid (RA)-responsive genes and induction of embryonal carcinoma cell differentiation by an RA receptor alpha (RAR alpha)-, RAR beta-, or RAR gamma-selective ligand in combination with a retinoid X receptor-specific ligand. Mol. Cell. Biol. *15*, 6481–6487.

Schuler, M., Ali, F., Metzger, E., Chambon, P., and Metzger, D. (2005). Temporally controlled targeted somatic mutagenesis in skeletal muscles of the mouse. Genesis *41*, 165–170.

Staiger, H., Staiger, K., Haas, C., Weisser, M., Machicao, F., and Haring, H.U. (2005). Fatty acid-induced differential regulation of the genes encoding peroxisome proliferator-activated receptor-gamma coactivator-1alpha and

-1beta in human skeletal muscle cells that have been differentiated in vitro. Diabetologia *48*, 2115–2118.

Tanaka, T., Yamamoto, J., Iwasaki, S., Asaba, H., Hamura, H., Ikeda, Y., Watanabe, M., Magoori, K., Ioka, R.X., Tachibana, K., et al. (2003). Activation of peroxisome proliferator-activated receptor delta induces fatty acid beta-oxidation in skeletal muscle and attenuates metabolic syndrome. Proc. Natl. Acad. Sci. USA *100*, 15924–15929.

Tanner, C.J., Barakat, H.A., Dohm, G.L., Pories, W.J., MacDonald, K.G., Cunningham, P.R., Swanson, M.S., and Houmard, J.A. (2002). Muscle fiber type is associated with obesity and weight loss. Am. J. Physiol. Endocrinol. Metab. *282*, E1191–E1196.

Voegel, J.J., Heine, M.J., Tini, M., Vivat, V., Chambon, P., and Gronemeyer, H. (1998). The coactivator TIF2 contains three nuclear receptor-binding motifs and mediates transactivation through CBP binding-dependent and -independent pathways. EMBO J. *17*, 507–519.

Wang, Y.X., Lee, C.H., Tiep, S., Yu, R.T., Ham, J., Kang, H., and Evans, R.M. (2003). Peroxisome-proliferator-activated receptor delta activates fat metabolism to prevent obesity. Cell *113*, 159–170.

Wang, Y.X., Zhang, C.L., Yu, R.T., Cho, H.K., Nelson, M.C., Bayuga-Ocampo, C.R., Ham, J., Kang, H., and Evans, R.M. (2004). Regulation of muscle fiber type and running endurance by PPARdelta. PLoS Biol. *2*, e294.

Wisloff, U., Najjar, S.M., Ellingsen, O., Haram, P.M., Swoap, S., Al-Share, Q., Fernstrom, M., Rezaei, K., Lee, S.J., Koch, L.G., and Britton, S.L. (2005). Cardiovascular risk factors emerge after artificial selection for low aerobic capacity. Science *307*, 418–420.

Wu, Z., Puigserver, P., Andersson, U., Zhang, C., Adelmant, G., Mootha, V., Troy, A., Cinti, S., Lowell, B., Scarpulla, R.C., and Spiegelman, B.M. (1999). Mechanisms controlling mitochondrial biogenesis and respiration through the thermogenic coactivator PGC-1. Cell *98*, 115–124.